Biophysical and pharmacological characterization of nicotinic cholinergic receptors in rat cochlear inner hair cells

María Eugenia Gómez-Casati[1], Paul A. Fuchs[2], Ana Belén Elgoyhen[1] and Eleonora Katz[1,3]

[1] *Instituto de Investigaciones en Ingeniería Genética y Biología Molecular, Consejo Nacional de Investigaciones Científicas y Técnicas – Universidad de Buenos Aires, Buenos Aires, Argentina*
[2] *Cochlear Neurotransmission Laboratory, Center for Hearing and Balance, Department of Otolaryngology – Head and Neck Surgery, Johns Hopkins University School of Medicine, Baltimore, MD, USA*
[3] *Departamento de Fisiología, Biología Molecular y Celular, Facultad de Ciencias Exactas y Naturales, Universidad de Buenos Aires, Buenos Aires, Argentina*

Before the onset of hearing, a transient efferent innervation is found on inner hair cells (IHCs). This synapse is inhibitory and mediated by a nicotinic cholinergic receptor (nAChR) probably formed by the α9 and α10 subunits. We analysed the pharmacological and biophysical characteristics of the native nAChR using whole-cell recordings from IHCs in acutely excised apical turns of the rat organ of Corti. Nicotine did not activate but rather blocked the acetylcholine (ACh)-evoked currents with an IC_{50} of 1 ± 0.1 μM. Antagonists of non-cholinergic receptors such as strychnine, bicuculline and ICS-205930 blocked ACh-evoked responses with an IC_{50} of 8.6 ± 0.8 nM, 59 ± 4 nM and 0.30 ± 0.02 μM, respectively. The IHC nAChR was both permeable to ($P_{Ca}/P_{Na} = 8 \pm 0.9$) and modulated by external Ca^{2+}. ACh-evoked currents were potentiated by Ca^{2+} up to 500 μM but were reduced by higher concentrations of this cation. Ba^{2+} mimicked the effects of Ca^{2+} whereas Mg^{2+} only blocked these currents. In addition, elevation of extracellular Ca^{2+} reduced the amplitude of spontaneous synaptic currents without affecting their time course. The receptor had an EC_{50} for ACh of 60.7 ± 2.8 μM in 0.5 mM Ca^{2+}. In the absence of Ca^{2+}, the EC_{50} for ACh increased, suggesting that potentiation by Ca^{2+} involves changes in the apparent affinity for the agonist. These pharmacological and biophysical characteristics of the IHC nAChR closely resemble those of the recombinant α9α10 nAChR, reinforcing the hypothesis that the functional nAChR at the olivocochlear efferent–IHC synapse is composed of both the α9 and α10 subunits.

(Resubmitted 23 March 2005; accepted after revision 21 April 2005; first published online 28 April 2005)
Corresponding author Eleonora Katz: INGEBI, Vuelta de Obligado 2490, 1428 Buenos Aires, Argentina. Email: ekatz@dna.uba.ar

In mammals, sound waves are converted into electrical signals by two types of mechanotransducer hair cells, inner and outer hair cells (IHCs and OHCs, respectively), present in the sensory epithelium of the cochlea. Adult IHCs are largely innervated by afferent nerve fibres, whereas OHCs are the main target of descending olivocochlear efferent fibres (Guinan, 1996). However, before the onset of hearing (around P12 in rats), olivocochlear efferent fibres transiently innervate immature IHCs prior to reaching their final OHC targets (Simmons *et al.* 1996; Pujol *et al.* 1998). Synaptic release from efferent neurones modulates the firing frequency of IHCs (Glowatzki & Fuchs, 2000) and could play a role in the establishment of the adult innervation to the cochlea (Walsh *et al.* 1998). Cholinergic innervation of vertebrate hair cells is brought about by Ca^{2+} entering through a nicotinic acetylcholine receptor (nAChR) and the subsequent activation of small conductance calcium-dependent potassium channels (SK channels) (Fuchs & Murrow, 1992*a*,*b*; Doi & Ohmori, 1993; Blanchet *et al.* 1996; Dulon & Lenoir, 1996; Evans, 1996; Fuchs, 1996; Nenov *et al.* 1996*b*; Dulon *et al.* 1998; Glowatzki & Fuchs, 2000; Oliver *et al.* 2000). In rat OHCs, it has also been recently shown that the inhibitory response mediated by the SK channels is boosted by Ca^{2+} released from a postsynaptic calcium storage organelle 'the synaptoplasmic cistern', subsequent to the activation of the nAChRs (Lioudyno *et al.* 2004).

Pharmacological and biophysical studies performed with the native cholinergic receptors present in mammalian OHCs (Doi & Ohmori, 1993; Erostegui *et al.* 1994*c*; Blanchet *et al.* 1996; Chen *et al.* 1996; Dulon & Lenoir, 1996; Evans, 1996; Nenov *et al.* 1996*b*; Oliver *et al.* 2000) and in chick short hair cells, equivalent to

 DOI: 10.1113/jphysiol.2005.087155

mammalian OHCs (Fuchs & Murrow, 1992*a*,*b*; McNiven *et al.* 1996), as well as cellular localization data (Elgoyhen *et al.* 1994; Park *et al.* 1997; Luo *et al.* 1998; Morley *et al.* 1998; Elgoyhen *et al.* 2001; Morley & Simmons, 2002), strongly suggest that the native OHC receptor is composed of both the $\alpha 9$ and $\alpha 10$ nicotinic subunits (Elgoyhen *et al.* 1994; Elgoyhen *et al.* 2001; Weisstaub *et al.* 2002). Both the native OHC nAChR and the recombinant $\alpha 9$ and $\alpha 9\alpha 10$ nAChR have a peculiar pharmacological profile. A hallmark of these receptors is that they are not activated by nicotine, the prototypic agonist of the family (Elgoyhen *et al.* 1994, 2001; Sgard *et al.* 2002). Studies performed with the recombinant $\alpha 9$ and $\alpha 9\alpha 10$ nAChRs expressed in *Xenopus laevis* oocytes (Katz *et al.* 2000; Weisstaub *et al.* 2002; Sgard *et al.* 2002) demonstrated that both receptors have a high Ca^{2+} permeability. There are other biophysical features, however, in which the $\alpha 9$ and $\alpha 9\alpha 10$ nAChR differ significantly, namely, voltage sensitivity, modulation by Ca^{2+} and desensitization pattern (Katz *et al.* 2000; Elgoyhen *et al.* 2001; Weisstaub *et al.* 2002). Aside from the fact that the $\alpha 9$ and $\alpha 10$ subunits are the only nicotinic subunits expressed by cochlear OHCs and IHCs (Elgoyhen *et al.* 1994, 2001; Park *et al.* 1997; Luo *et al.* 1998; Morley *et al.* 1998; Morley & Simmons, 2002), studies with mice carrying a null mutation in the *Alpha9* gene showed that these $\alpha 9$ knock-out mice are functionally de-efferented, thus indicating that the $\alpha 9$ subunit is a key component of the native receptor (Vetter *et al.* 1999). Moreover, we have recently shown that the developmental loss of functional nAChRs at the transient olivocochlear efferent–IHC synapse is strongly correlated with diminished expression of the $\alpha 10$ subunit, thus supporting a key role for this subunit in the functional expression of hair cell nAChRs as well (Katz *et al.* 2004).

In the present work we characterized pharmacological and biophysical features of the native nAChR present at the olivocochlear efferent–IHC synapse prior to the onset of hearing. We show that these characteristics of the IHC nAChR studied in isolation from the SK2 channels are very similar to those described for the recombinant $\alpha 9\alpha 10$ nAChR, providing further evidence that the native IHC functional receptor is composed of both the $\alpha 9$ and $\alpha 10$ subunits.

Methods

Animal procedures and isolation of the organ of Corti

Sprague-Dawley rats at postnatal ages 9–11 (P9–11; day of birth was considered P0) were anaesthetized with an I.P. injection of sodium pentobarbital. Animals were decapitated after assessing that a deep anaesthetic state had been obtained (by observing the lack of tail flick following tail pinch, and lack of eye blink response following a corneal touch). All experimental protocols were carried out in accordance with the National Institutes of Health *Guide for the Care and Use of Laboratory Animals* (NIH Publications no. 80-23) revised 1978. Apical turns of the organ of Corti were excised as previously described (Glowatzki & Fuchs, 2000) and used within 3 h. Cochlear preparations were mounted under an Axioskope microscope (Zeiss, Oberkochem, Germany) and viewed with differential interference contrast (DIC) using a 63× water immersion objective and a camera with contrast enhancement (Hamamatsu C2400-07, Hamamatsu City, Japan).

Electrophysiological recordings

Methods to record from IHCs were essentially as described (Glowatzki & Fuchs, 2000). Briefly, IHCs were identified visually, then by their whole-cell capacitance (7–12 pF) and by their characteristic voltage-dependent Na^+ and K^+ currents, including at older ages a fast-activating K^+ conductance (Kros *et al.* 1998). Some cells were removed to access IHCs, but mostly the pipette moved through the tissue using positive fluid flow to clear the tip.

Currents in IHCs were recorded in the whole-cell patch-clamp mode using an Axopatch 200B amplifier (Axon Instruments, Union City, CA, USA), low-pass filtered at 2–10 kHz and digitized at 5–20 kHz with a Digidata 1200 board (Axon Instruments). Recordings were made at room temperature (22–25°C). Glass pipettes, 1.2 mm i.d., had resistances of 7–10 MΩ.

Solutions

The cochlear preparation was continuously superfused ($\sim$0.5 ml min^{-1}) with an extracellular solution with an ionic composition similar to that of the perilymph (mM): 144 NaCl, 5.8 KCl, 1.3 $CaCl_2$, 0.9 $MgCl_2$, 0.7 NaH_2PO_4, 5.6 D-glucose and 10 Hepes buffer; pH was adjusted 7.4 with NaOH. For the Ca^{2+} permeability experiments and for the modulation of spontaneous synaptic currents by Ca^{2+}, the extracellular solution was as follows (mM): 100 NaCl, 5.8 KCl, 1.3 mM $CaCl_2$, 0.9 $MgCl_2$, 5.6 D-glucose and 10 Hepes buffer; pH 7.4 (osmolality was adjusted to 300–320 mosmol kg^{-1} with sucrose $\sim$26 g l^{-1}).

Solutions containing different divalent cation concentrations, with or without ACh, were applied by a gravity-fed multichannel glass pipette ($\sim$150 μm tip diameter) positioned about 300 μm from the recorded IHC. All working solutions applied via the gravity-fed multi-channel glass pipette, except for those designed to study the effects of Mg^{2+} on the ACh-evoked responses, were made up in a saline containing 0.5 mM Ca^{2+} (unless otherwise stated) and without Mg^{2+}, so as to optimize the experimental conditions for measuring currents flowing through the $\alpha 9\alpha 10$ receptors (Weisstaub *et al.* 2002). Working solutions contained (mM): 144 NaCl, 5.8 KCl, 0.5 $CaCl_2$, 0.7 NaH_2PO_4, 5.6 D-glucose, and 10 Hepes buffer; pH was adjusted 7.4 with NaOH. For the

Ca^{2+} permeability experiments and for the modulation of spontaneous synaptic currents by Ca^{2+}, the working solution was as follows (mM): 100 NaCl, 5.8 KCl, 0–10 mM $CaCl_2$, 5.6 D-glucose, and 10 Hepes buffer; pH 7.4 (osmolality was adjusted to 300–320 mosmol kg^{-1} with sucrose ~26 g l^{-1}).

The pipette solutions contained the following (mM). (1) KCl-EGTA saline (for recording the combined nAChR + SK response): 135 KCl, 3.5 $MgCl_2$, 0.1 $CaCl_2$, 5 ethyleneglycol-bis(β-aminoethyl ether)-*N*,*N*,*N*′,*N*′-tetraacetic acid (EGTA), 5 Hepes buffer, 2.5 Na_2ATP, pH adjusted to 7.2 with KOH. (2) KCl-BAPTA saline (for recording the isolated nAChR response): to preclude the activation of SK currents by Ca^{2+}, in some experiments EGTA in the pipette solution was replaced by 10 mM of the fast calcium chelator 1,2-bis(2-aminophenoxy)ethane-*N*,*N*,*N*′,*N*′-tetraacetic acid (BAPTA); 135 KCl, 3.5 $MgCl_2$, 0.1 $CaCl_2$, 10 BAPTA, 5 Hepes buffer, 2.5 Na_2ATP, pH adjusted to 7.2 with KOH. In order to minimize further the contribution of SK channel currents, in addition to using BAPTA in the pipette solution, the SK channel blocker apamin (1–10 nM) (Kohler *et al.* 1996) was added to the external working solutions.

In the experiments designed to study the voltage dependence of the nAChR currents and/or the changes in the current reversal potential, KCl in the KCl-BAPTA saline was replaced by either CsCl or Cs-gluconate, to eliminate voltage-dependent K^+ currents (Kros *et al.* 1998). The osmolality of intracellular solutions ranged between 270 and 290 mosmol kg^{-1}. Spontaneous synaptic currents were recorded immediately after rupturing into the cell, in the extracellular saline containing 0.5 mM Ca^{2+} and with a recording pipette containing either a KCl-EGTA (combined nAChR + SK synaptic currents) or a KCl-BAPTA saline solution (isolated nAChR synaptic currents).

Evaluation of divalent cation permeability

For these experiments, ionic currents were elicited by ACh in IHCs held at different membrane potentials (−40 to +30 mV, in 5 mV steps). The relative calcium to sodium permeability (P_{Ca}/P_{Na}) was evaluated by computing the reversal potential (E_{rev}) of ACh-evoked currents upon changing the external Ca^{2+} concentration from 0.1 mM to 10 mM while keeping a fixed Na^+ concentration of 100 mM. Data were then fitted by the constant field Goldman-Hodgkin-Katz (GHK) voltage equation extended to include divalent cations (Jan & Jan, 1976). Our assumptions were that Na^+, K^+ and Cs^+ are equally permeant and that Cl^- is impermeant through this channel; in addition we made no allowance for the effect of surface charge on the value of P_{Ca}/P_{Na} (Mayer & Westbrook, 1987). Thus, taking into account the permeability to K^+, Na^+ and Ca^{2+}, the E_{rev} was evaluated to be:

$$E_{rev} = RT/F \ln(-b + (b^2 - 4ac)^{1/2}/2a)$$

in which:

$$a = [K^+]_i + 4P_{Ca}/P_K[Ca^{2+}]_i + P_{Na}/P_K[Na^+]_i,$$

$$b = ([K^+]_i - [K^+]_o + P_{Na}/P_K([Na^+]_i - [Na^+]_o),$$

$$c = -[K^+]_o - P_{Na}/P_K[Na^+]_o - 4P_{Ca}/P_K[Ca^{2+}]_o,$$

where P_K, P_{Na} and P_{Ca} are the membrane permeabilities to K^+, Na^+ and Ca^{2+}, respectively (under our experimental conditions $[K^+]_i$ was replaced by $[Cs^+]_i$); R is the molar gas constant, F is the Faraday constant, and T is absolute temperature (RT/F is 25.3 mV at 20°C). For comparison with previous data on the recombinant rat $\alpha9$ and $\alpha9\alpha10$ nAChR (Katz *et al.* 2000; Weisstaub *et al.* 2002) and their recombinant human orthologues (Sgard *et al.* 2002), we used ionic concentrations and not ionic activities in our calculations.

Evaluation of the modulation of the native receptor by divalent cations

The effects of extracellular Ca^{2+}, Ba^{2+} and Mg^{2+} on the ionic currents through the nAChR receptor were studied by measuring the amplitudes of the responses to 100 μM ACh upon varying the concentration of these cations from 0 to 10 mM. In all cases the IHC under study was preincubated for 1 min with a saline containing the concentration of divalent cations to be tested.

Amplitude values obtained at each concentration were normalized to that obtained in the same cell at a 0.5 mM concentration of the divalent cation being studied. Values from different IHCs were averaged and expressed as the mean ± S.E.M.

Evaluation of inhibition

The IC_{50} values for the inhibition by Mg^{2+} and other antagonists (nicotine, strychnine, ICS-205930 and bicuculline) were evaluated in the presence of 0.5 mM Ca^{2+} and calculated by:

$$I/I_{max} = 1/(1 + 10^{(\log IC_{50} - X)n_H}),$$

where I is the current obtained at the different concentrations of the antagonist, I_{max} is the current obtained in the absence of antagonist, X is the logarithm of the antagonist concentration and n_H is the Hill coefficient. IC_{50} values were obtained for each IHC and then averaged. Data are presented as means ± S.E.M.

To study the inhibitory effects of Mg^{2+} or the other antagonists, in all cases the IHC under study was preincubated for 1 min with the same concentration of the antagonist to be tested.

Evaluation of the effect of divalent cations on the affinity of the nAChR for ACh

To evaluate changes in affinity and maximal response to ACh, concentration–response curves to ACh were carried out in the same IHCs at nominally 0 and 0.5 mM Ca^{2+}. Values were normalized to the maximum obtained at 0.5 mM Ca^{2+}. EC_{50} values were calculated by:

$$I/I_{max} = 1/(1 + 10^{(\log EC_{50} - X)n_H}),$$

Data analysis

For *I–V* curves and voltage dependence of divalent cation block, voltages were corrected for liquid junction potentials (−4 mV and −17 mV for the KCl (or CsCl) and Cs-gluconate intracellular solutions, respectively). Voltages were not corrected for the voltage drop across the uncompensated series resistance. Spontaneous synaptic currents were analysed with Minianalysis (Synaptosoft, Jaejin Software, Leonia, NJ, USA) and were identified using a search routine for event detection and confirmed by eye. τ_{decay} values were fitted with a monoexponential. Statistical analyses were carried by ANOVA followed by Tukey's test for multiple comparisons or by Student's two-tailed *t* test (when only two populations of data were compared). In both cases $P < 0.05$ was considered significant.

Materials

ACh-chloride, BAPTA free acid, Na_2ATP, strychnine-HCl (–)-bicuculline methbromide, ICS-205930-HCl, (–)-nicotine-di-*d*-tartrate, apamin and all other reagents were from Sigma Chemical Co. (St Louis, MO, USA). BAPTA and Na_2ATP were dissolved at the moment of preparing the intracellular solutions. All other drugs were dissolved in distilled water as 1–10 or 100 mM stocks and stored in aliquots at −20°C.

Results

Voltage sensitivity, pharmacological profile and desensitization pattern of the isolated nAChR current

Application of 100 μM ACh, in the presence of a low Ca^{2+}–Mg^{2+} free saline solution in the bath and using a KCl-EGTA-based pipette solution, caused inward currents in postnatal (P9–11) IHCs voltage clamped at −90 mV and outward currents at −50 and −30 mV. The current–voltage relation (Fig. 1*A*, nAChR + SK) was bell shaped and the average reversal potential, −67.6 ± 4.2 mV ($n = 5$), was near the potassium equilibrium potential (E_K, −82 mV). Under these conditions, ACh-activated currents were mediated by a combined flux of cations through the α9α10-containing nAChR and a K^+ flux through calcium-dependent SK channels. Negative to E_K, at −90 mV, the ACh-activated inward current is mediated by current flow through both the nAChR channel and the SK channel whereas at voltages between E_K and 0 mV, the outward current flows through SK channels. In order to isolate the nAChR current, the calcium-activated SK current was blocked by using the calcium chelator BAPTA (10 mM) instead of EGTA in the pipette solution plus the addition of 1 nM apamin, a specific SK channel blocker (Köler *et al.* 1996), to the bath solution. Under these conditions the residual currents reversed nearer to 0 mV ($E_{rev} = -10.7 \pm 1.6$ mV; $n = 3$), and the *I–V* relation was more linear (Fig. 1*A*, nAChR).

We characterized the effects of drugs reported to block both the recombinant α9α10 nAChRs and OHC native receptors (Elgoyhen *et al.* 1994; Erostegui *et al.* 1994*c*; Chen *et al.* 1996; Rothlin *et al.* 1999; Verbitsky *et al.* 2000; Elgoyhen *et al.* 2001), on the isolated nAChR-mediated current in IHCs. Nicotine is the prototypic cholinergic agonist of nicotinic receptors, except for the recombinant α9 and α9α10 receptors on which it behaves as an antagonist (Elgoyhen *et al.* 1994, 2001). When tested in IHCs, nicotine did not evoke currents itself but rather blocked the ACh-evoked responses in a reversible manner with an IC_{50} of 1 ± 0.1 μM ($n = 3$–5 cells; Fig. 1*B*). Another pharmacological hallmark of the recombinant α9 and α9α10 nAChRs is that they are potently blocked by antagonists of non-cholinergic receptors such as strychnine (glycine receptors), bicuculline (γ-aminobutyric acid type A receptors), and ICS-205930 (ligand gated serotonin receptors) (Rothlin *et al.* 1999; Elgoyhen *et al.* 2001). As illustrated by the concentration–response curves in Fig. 1*B*, these three compounds blocked ACh-evoked responses in IHCs with an IC_{50} of 8.6 ± 0.8 nM for strychnine ($n = 3$–5 cells), 59 ± 4 nM for ICS-205930 ($n = 4$ cells) and 0.3 ± 0.02 μM for bicuculline ($n = 3$–5 cells). The effects of all four drugs were readily reversed by superfusing the preparation with normal saline solution (Fig. 1*C*).

We have previously shown that homomeric α9 and heteromeric α9α10 channels differed in their desensitization kinetics. Whereas responses to ACh in α9α10-expressing oocytes are markedly reduced upon the continuous (1 min) or intermittent (10 s at 0.025 Hz) application of the agonist, in α9-expressing oocytes, ACh-evoked responses do not desensitize with either protocol (Elgoyhen *et al.* 2001). Figure 2 shows that the native nAChR in IHCs also desensitized upon either the continuous (1 min) or intermittent (10 s at 0.05 Hz) application of ACh. In the continuous presence of 1 mM ACh, currents through the nAChR decayed with a time constant of 13.8 ± 0.5 s ($n = 4$, Fig. 2*A* and *C*). In the case of intermittent application of the agonist, peak amplitudes decayed with a time constant of 37.9 ± 4.2 s ($n = 3$, Fig. 2*B* and *D*). It must be borne in mind that the decay time constant values obtained for desensitization might be flawed by the limitation imposed by the slow perfusion of the intact cochlear coil. Solution exchange around the cell, as evaluated by the change in holding current when

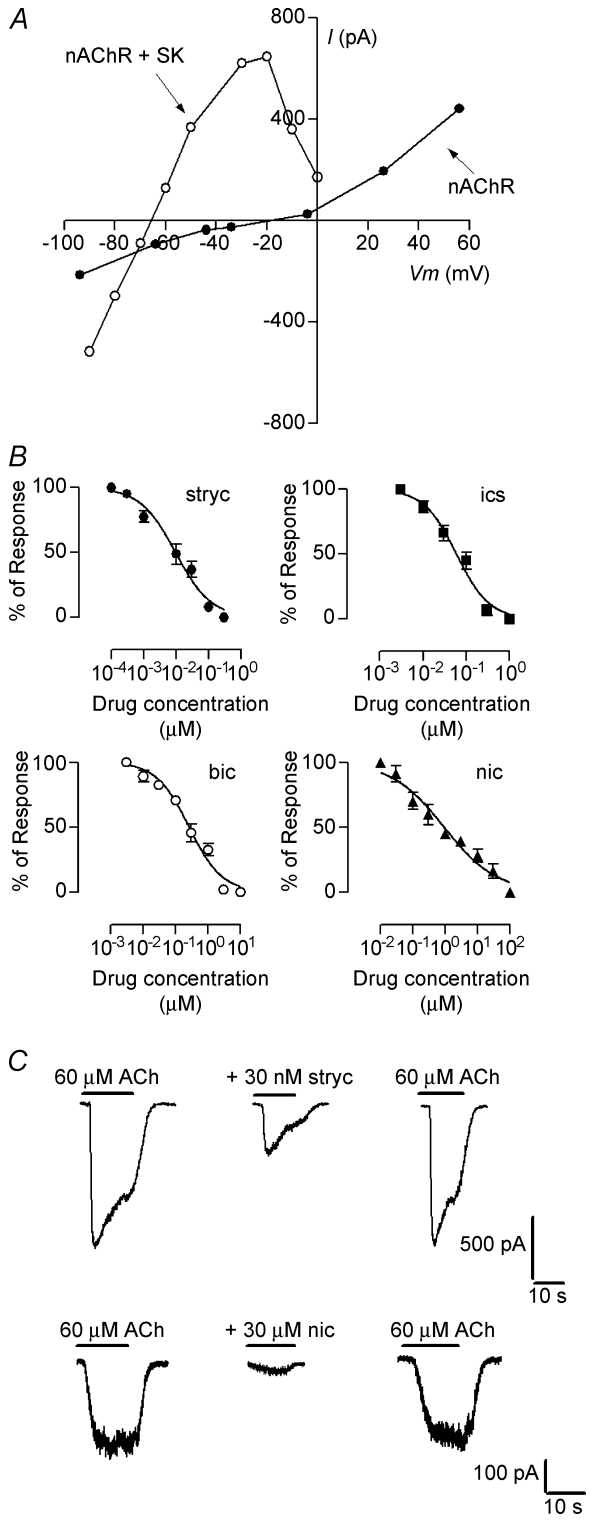

Figure 1. Voltage sensitivity and pharmacological profile of the native IHC nAChR

A, representative *I–V* relationships illustrating the voltage dependence of the combined (nAChR + SK, KCl-EGTA saline solution in the recording pipette) and isolated responses (nAChR; CsCl-BAPTA saline solution in the recording pipette plus 1 nM apamin in the extracellular solution) evoked by exogenously applied ACh (100 μM).
B, concentration–response curves in the presence of different antagonists: strychnine (IC_{50}: 8.6 ± 0.8 nM; n_H: 0.65 ± 0.1); ICS-205930 (IC_{50}: 59 ± 4 nM; n_H:1.2 ± 0.2), bicuculline (IC50: 0.3 ± 0.02 μM; n_H: 0.9 ± 0.1) and nicotine (IC_{50}: 1 ± 0.1 μM; n_H: 0.5 ± 0.1). Responses were normalized to the response obtained with 60 μM ACh in the absence of antagonist. *C*, representative records of currents evoked by 60 μM ACh in the absence or presence of different concentrations of only two of the antagonists used (strychnine and nicotine). In all cases the effects of the antagonists were completely reversed by washing the cells in a saline solution without antagonist. In *A* and *B*, the records and data points for *I–V* and concentration–response curves are representative of results obtained in 3–6 IHCs. In *B* and *C* all ACh responses were elicited in IHCs voltage clamped at –90 mV.

changing form 5.8 mM to 40 mM KCl, is complete in around 1–3 s according to the position of the perfusion pipette in relation to the cell under study (data not shown, see Glowatzki & Fuchs, 2000; Katz *et al.* 2004). This slow ACh application, which is similar to the slow perfusion method used to study the recombinant $\alpha9$ and $\alpha9\alpha10$ in *Xenopus* oocytes (see Elgoyhen *et al.* 2001), should lead to an underestimation of the peak current as desensitization would start before the peak is reached, and therefore to an underestimation of desensitization itself.

Ca^{2+} permeability of the IHC nAChR

The inhibitory sign of the cholinergic olivocochlear synapse depends upon Ca^{2+} influx through the nAChR and the subsequent activation of SK channels (Fuchs & Murrow, 1992*a*; Evans, 1996; Dulon *et al.* 1998; Blanchet *et al.* 1996, Glowatzki & Fuchs, 2000; Oliver *et al.* 2000; Gomez-Casati *et al.* 2004). It has been previously shown that both the $\alpha9$ and $\alpha9\alpha10$ recombinant receptors are highly permeable to Ca^{2+} (Katz *et al.* 2000; Weisstaub *et al.* 2002; Sgard *et al.* 2002). In order to know the extent to which calcium permeates the native IHC nAChR, we studied the variation in the reversal potential of the ACh-evoked currents upon variation of the external Ca^{2+} concentration while keeping constant the Na^+ concentration. Figure 3*A* shows representative *I–V* curves in the presence of different Ca^{2+} concentrations. As expected for a Ca^{2+}-permeable channel, increasing the extracellular Ca^{2+} concentration caused a significant positive shift in E_{rev}. In Fig. 3*B*, averaged E_{rev} data from different IHCs are plotted against the different Ca^{2+} concentrations employed. P_{Ca}/P_{Na} was 8 ± 0.9 ($n = 6$ cells) as estimated by the extended constant field equation (see Methods). In 10 mM external Ca^{2+}, we found that there was some residual activation of SK channels even though we used 10 mM BAPTA in the pipette and 1 nM apamin in the external solution (data not shown). Therefore, for the permeability experiments we

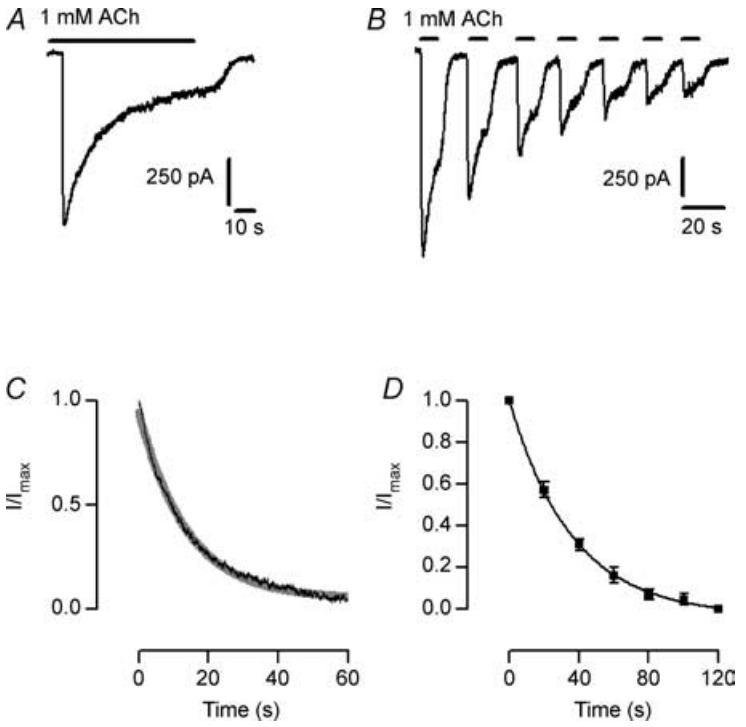

Figure 2. Desensitization pattern of the native IHC nAChR
Representative records illustrating that ACh-evoked responses desensitize both for the continued (*A*) and intermittent application of ACh (*B*), obtained in 3–4 IHCs voltage clamped at –90 mV. *C*, plot of I/I_{max} *versus* time during the continuous application of 1 mM ACh. Illustrated is the average trace obtained from 4 IHCs. The grey line is a monoexponential fit to the data ($\tau_{decay} = 13.8 \pm 0.5$ s). *D*, plot of I/I_{max} *versus* time during the intermittent application of ACh. Data points are the average current amplitudes ($n = 3$ IHCs) at each subsequent ACh pulse. Data were fitted by a monoexponential decay equation; $\tau_{decay} = 37.9 \pm 4.2$ s.

used 10 nM apamin in all the Ca^{2+} concentrations tested. Notwithstanding, there still could be a small contribution of SK channels to the total ACh-evoked current in 10 mM Ca^{2+}. If this were the case, we would be underestimating the shift in E_{rev} upon changing to this highest Ca^{2+} concentration and thus underestimating P_{Ca}/P_{Na}.

Modulation of the native IHC nAChR by Ca^{2+}, Ba^{2+} and Mg^{2+}

We have previously shown that the homomeric $\alpha 9$ nAChR is strongly blocked by micromolar concentrations of either Ca^{2+} or Ba^{2+} in the extracellular solution (Katz *et al.* 2000), whereas the heteromeric $\alpha 9\alpha 10$ receptor

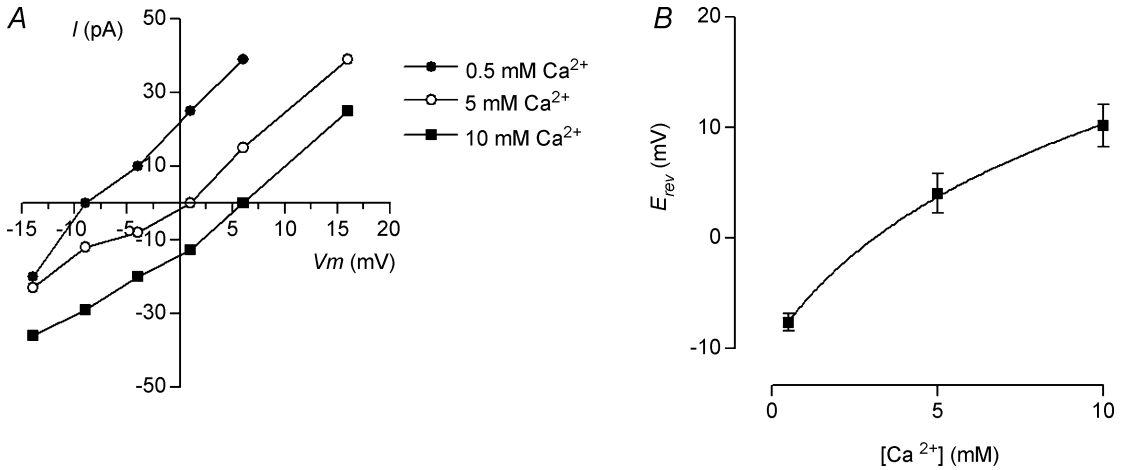

Figure 3. Ca^{2+} permeability of the native nAChR
A, representative *I–V* curves obtained in the presence of different external Ca^{2+} concentrations (0.5, 5 and 10 mM) and a fixed extracellular Na^{+} concentration (100 mM). Note that as expected for a Ca^{2+} permeable channel, E_{rev} shifted to more positive potentials as the Ca^{2+} concentration was increased. *B*, plot of E_{rev} (each data point is the mean ± S.E.M., $n = 6$ IHCs) *versus* the external Ca^{2+} concentration. Data were fitted with the GHK voltage equation extended to include divalent cations (see Methods) and the estimated P_{Ca}/P_{Na} was 8 ± 0.9.

shows a more complex response upon variation of these divalent cations. At micromolar extracellular Ca^{2+} or Ba^{2+} concentrations, ACh-evoked responses through this receptor are potentiated, but at concentrations above 0.5 mM responses are strongly reduced (Elgoyhen *et al.* 2001; Weisstaub *et al.* 2002). As the $\alpha9$ and $\alpha9\alpha10$ nAChRs are blocked by Mg^{2+} (Katz *et al.* 2000; Weisstaub *et al.* 2002), in order to investigate the modulation by Ca^{2+} and Ba^{2+} of the native IHC nAChR we chose to vary their concentration without compensation by other divalent cations.

Figure 4*A* shows representative responses of IHCs to the exogenous application of 100 μM ACh in the presence of increasing concentrations of Ca^{2+} (0, 0.1, 0.5, 1 and 3 mM) in the extracellular solution. Currents were negligible in a Ca^{2+}-free solution, were potentiated by micromolar concentrations of Ca^{2+} and were inhibited by Ca^{2+} concentrations above 0.5 mM. The bar graph in Fig. 4*B* illustrates the averaged data obtained from different IHCs. Current amplitudes at different Ca^{2+} concentrations in each IHC were normalized with respect to those obtained at 0.5 mM in the same cell. A one-way ANOVA indicated that differences in mean current amplitudes in 0, 0.1, 1 and 3 mM Ca^{2+} were significant with respect to the mean amplitude obtained at 0.5 mM Ca^{2+} ($P < 0.001$). When Ba^{2+} substituted for Ca^{2+} in the external solution (Figs 4*C* and *D*), the same dual effect, potentiation and block, was observed. The one-way ANOVA indicated that differences in mean current amplitudes between 0, 0.1, 3 and 5 mM Ba^{2+} were significant with respect to the mean amplitude obtained at 0.5 mM Ba^{2+} ($P < 0.001$).

In order to evaluate the effects of Mg^{2+} on the native nAChR, the same type of experiments as those shown in Fig. 4 were carried out on IHCs superfused with an

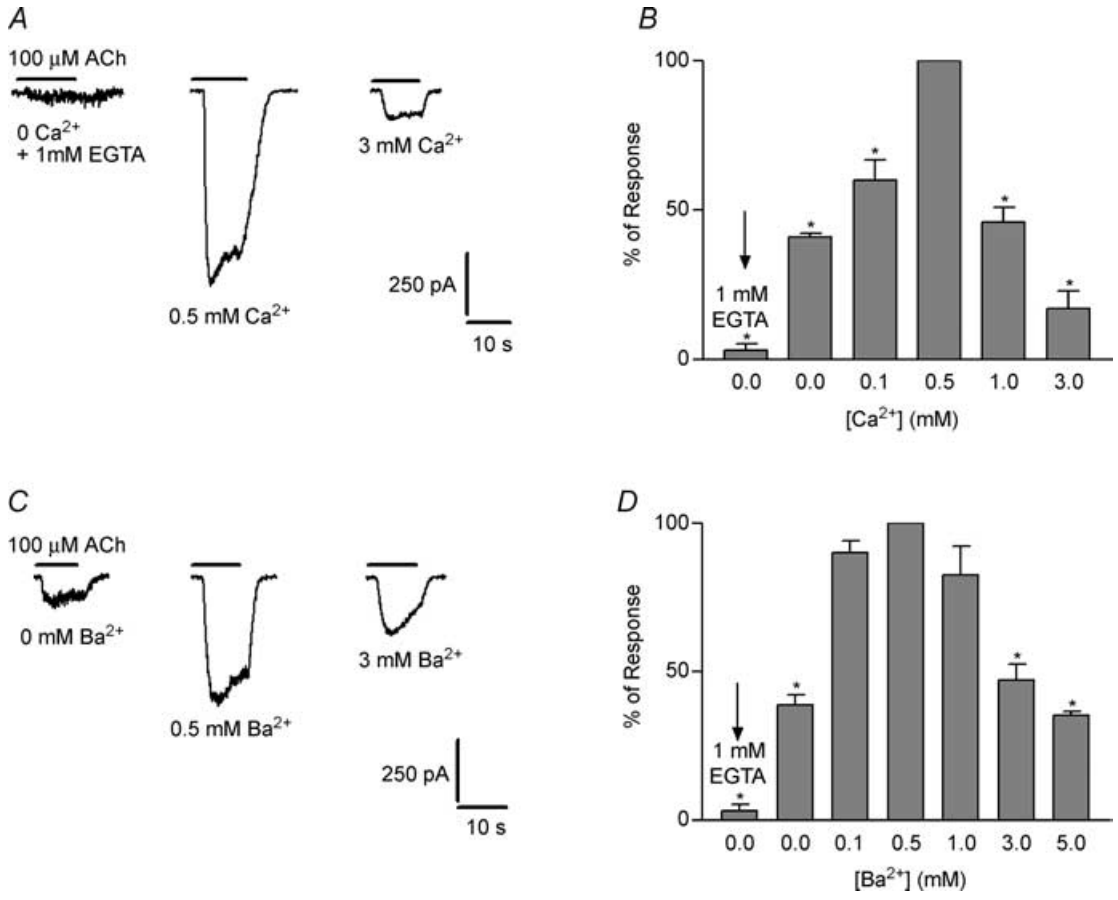

Figure 4. Modulation of the isolated nAChR by Ca^{2+} and Ba^{2+}
A, representative records of currents evoked by 100 μM ACh in the presence of different concentrations of Ca^{2+}. *B*, bar graph illustrating that in the physiological range Ca^{2+} both potentiates and diminishes ionic currents through the nAChR studied in isolation from the SK channels. *C* and *D*, the same as *A* and *B* but in the presence of Ba^{2+} instead of Ca^{2+}. Asterisks indicate that the amplitudes obtained at a given Ca^{2+} or Ba^{2+} concentration were significantly different from that obtained at 0.5 mM for either cation. All experiments were carried out in IHCs voltage clamped at −90 mV ($n = 3$–7 cells). Mean current amplitudes used to normalize the data in the bar graphs were: -752.4 ± 49.6 pA ($n = 7$ IHCs) and -480 ± 99 pA ($n = 7$ IHCs) in 0.5 mM Ca^{2+} and 0.5 mM Ba^{2+}, respectively. Slope conductances at −90 mV were 8.4 ± 0.5 nS and 5.3 ± 1.1 nS in 0.5 mM Ca^{2+} and 0.5 mM Ba^{2+}, respectively.

external solution in which Ca^{2+} was replaced by Mg^{2+}. Figure 5 shows representative traces of the responses obtained in a nominally Ca^{2+}-free solution (no added buffer) containing increasing concentrations of Mg^{2+}. As illustrated in Fig. 5*A*, upon increasing the concentration of Mg^{2+} to 0.1 and 0.3 mM, responses to 100 μM ACh were not potentiated but strongly reduced. Even at concentrations < 0.1 mM, no potentiation of ACh-evoked responses were observed (data not illustrated). The reduction in the current amplitude was rapidly reversed upon superfusing the cells with a saline solution without Mg^{2+}. The concentration–response curve in Fig. 5*B*, performed in a solution containing 0.5 mM Ca^{2+}, shows that Mg^{2+} blocked the IHC nAChR with an IC_{50} of 0.2 ± 0.01 mM (data were pooled from $n = 3$–11 IHCs).

Mechanism of Ca^{2+} potentiation

To evaluate whether changes in the apparent affinity of ACh for the native IHC receptor could account for the potentiation by Ca^{2+}, concentration–response curves to ACh were performed at two different Ca^{2+} concentrations. Figure 6 illustrates these results for IHCs superfused with either nominally calcium-free or 0.5 mM Ca^{2+} saline. Under these conditions the EC_{50} values were 160 ± 6 μM ($n = 4$ IHCs) and 60.7 ± 2.8 μM ($n = 3$–7 IHCs) for 0 and 0.5 mM Ca^{2+} saline, respectively. These differences in the EC_{50} show that in a nominally Ca^{2+}-free saline solution the apparent affinity of the IHC nAChR receptor for the agonist was lower than that observed in the presence of 0.5 mM Ca^{2+}. The maximal response obtained in zero Ca^{2+} was not significantly different from that obtained in 0.5 mM Ca^{2+} (for example, in the same IHC the amplitude of currents evoked by 1 mM ACh was -746 pA in 0 Ca^{2+} and -772 pA in 0.5 mM Ca^{2+}; see concentration–response curves in Fig. 6 for average responses in all IHCs tested under both conditions), indicating that at high ACh concentrations, the response of the native receptor becomes independent of Ca^{2+} in the external medium.

Mechanism of block by divalent cations

We studied the mechanism of divalent cation block using Ba^{2+} instead of Ca^{2+} to preclude the contribution of SK channels. Representative *I–V* curves in the presence of 0.5 and 5 mM Ba^{2+} (Fig. 7*A*) show that block by Ba^{2+} was sensitive to membrane voltage being more pronounced at hyperpolarized than at depolarized potentials. This effect can be better appreciated by the conductance *versus* voltage plot (ratios of conductance in 5 mM Ba^{2+}/conductance in 0.5 mM Ba^{2+}) where it can be observed that conductance in 5 mM Ba^{2+} is significantly lower than that in 0.5 mM Ba^{2+} at hyperpolarized potentials (Fig. 7*B*). In agreement with this, the bar graph in Fig. 7*C* shows that rectification of the *I–V* curve was significantly greater in higher barium concentrations. The ratio of current amplitudes at +60 and -90 mV ($+43$ and -107 mV when corrected for liquid junction potential) was 2.3 ± 0.1 ($n = 14$ IHCs) and 4.2 ± 0.4 ($n = 12$ IHCs) for 0.5 mM and 5 mM Ba^{2+}, respectively.

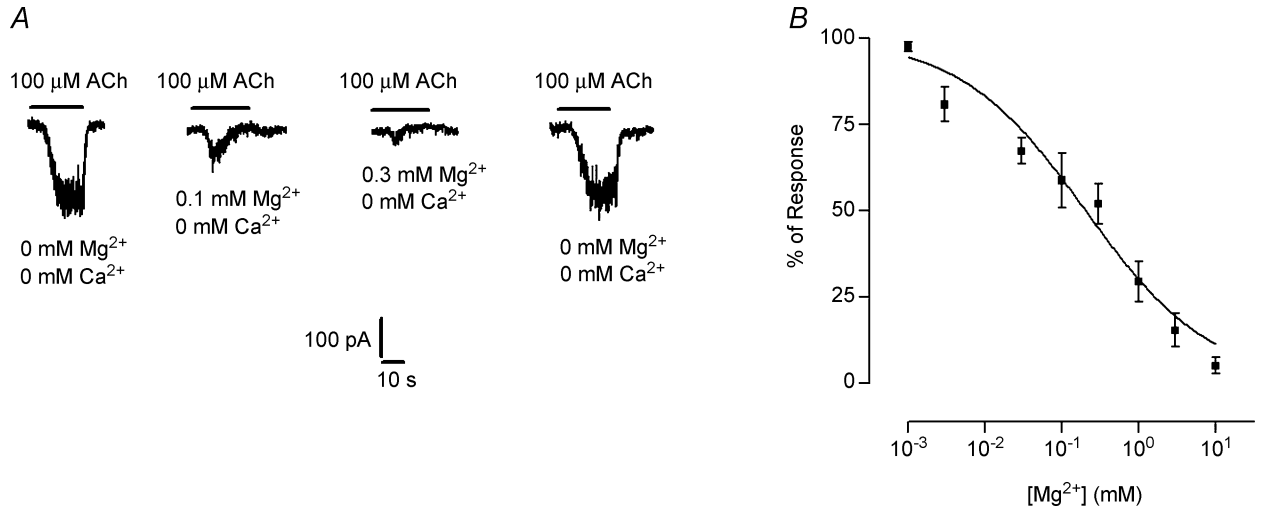

Figure 5. Effects of Mg^{2+} on the isolated nAChR currents
A, representative records of currents evoked by 100 μM ACh in the absence of Ca^{2+}, with (0.1 and 0.3 mM) or without Mg^{2+}. Note that micromolar concentrations of Mg^{2+} do not potentiate but strongly reduce these currents. *B*, concentration–response curve obtained in the presence of 100 μM ACh, 0.5 mM Ca^{2+} and increasing concentrations of Mg^{2+}. The amplitudes of the ACh-evoked currents in the presence of the different Mg^{2+} concentrations were normalized to the values obtained in the absence of this cation. Mg^{2+} blocked the nAChR with an IC_{50} of 0.21 ± 0.01 mM, $n_H = 0.53 \pm 0.06$ (data were pooled from 3 to 11 IHCs). All experiments were carried out in IHCs voltage clamped at -90 mV.

Ca^{2+} modulation of isolated nAChR synaptic currents

It has been reported that changes in extracellular Ca^{2+} acting on nAChRs modify spontaneous cholinergic synaptic currents in sympathetic ganglion neurones (Amador & Dani, 1995). In the cochlear preparation used in the present study, spontaneous inhibitory postsynaptic currents (IPSCs) due to efferent synaptic transmission were observed in IHCs superfused with a saline solution containing 0.5 mM Ca^{2+} and recorded with a patch pipette containing a KCl-EGTA based saline solution (see Methods). Under this condition, synaptic currents are composed of ions flowing through both the nAChRs and the SK channels. As previously described (Glowatzki & Fuchs, 2000), at voltages between −70 and −50 mV these IPSCs have two components (Fig. 8*A*, upper record and see also Fig. 1 in Glowatzki & Fuchs, 2000), a fast inward component due to the inward flux of Na^+ and Ca^{2+} through the nAChR and a more delayed and longer lasting outward component due to the opening of the calcium activated SK channels. The resting potential of IHCs is positive to E_K and therefore the functional significance of efferent activity is to hyperpolarize the IHC. These spontaneous synaptic currents were inward at −90 mV with mean amplitude of -28.4 ± 1 pA. IPSCs rose rapidly (time to peak 9.6 ± 0.7 ms) and decayed more slowly (τ_{decay} 30.3 ± 1.9 ms, $n = 52$ events, 6 cells, Fig. 8*A* and *B*). At −30 mV, IPSCs were outward with a mean amplitude

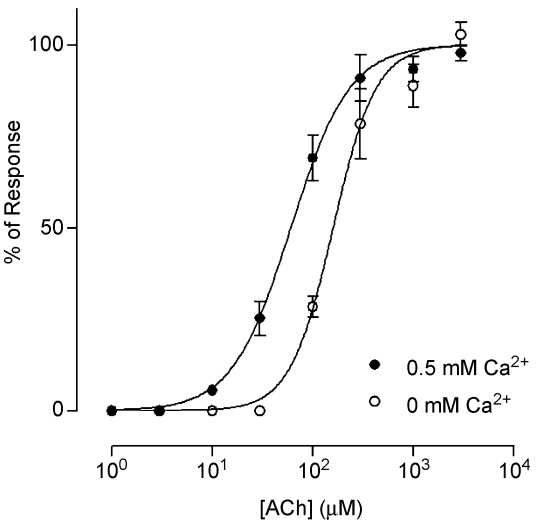

Figure 6. Mechanism of Ca^{2+} potentiation
Concentration–response curves performed in 0 and 0.5 mM Ca^{2+} are shown. A significant leftward shift in the EC_{50} upon increasing the Ca^{2+} concentration to 0.5 mM (EC_{50}: 160 ± 6 μM and 60.7 ± 2.8 μM for 0 and 0.5 mM Ca^{2+}, respectively) was observed, thus suggesting that potentiation by Ca^{2+} involves changes in the apparent affinity of the native receptor for ACh. Responses were normalized to the maximal value obtained in 0.5 mM Ca^{2+}. Data were pooled from 3 to 7 IHCs. All experiments were carried out in IHCs voltage clamped at −90 mV.

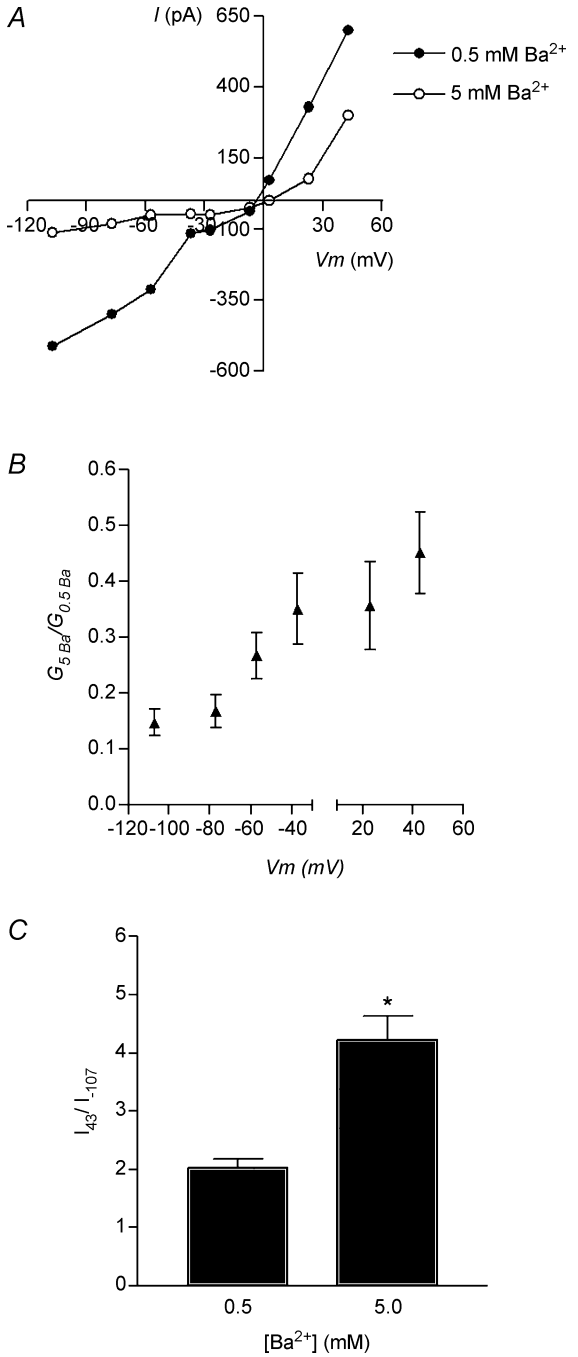

Figure 7. Voltage dependence of divalent cation block
A, representative *I–V* curves obtained at 0.5 and 5 mM Ba^{2+} in the extracellular solution. Note that in 5 mM Ba^{2+} the nAChR passes much less inward than outward current. *B*, the ratio of chord conductance in 5 mM Ba^{2+} with respect to that in 0.5 mM Ba^{2+} plotted against membrane voltage, shows that block by Ba^{2+} is much more effective at hyperpolarized than at depolarized potentials. The break in the *x*-axis corresponds to the data points that are close to or at the reversal potentials for the currents through the nAChR in 0.5 and 5 mM Ba^{2+}. *C*, the ratio of current amplitudes at depolarized potentials (+43 mV) with respect to that at hyperpolarized potentials (−107 mV) shows that outward rectification is significantly higher in ACh-evoked currents elicited in the presence of 5 mM Ba^{2+} than those obtained in 0.5 mM Ba^{2+}. Data were pooled from 12 to 14 IHCs.

of 33.2 ± 1.7 pA, time to peak $= 12 \pm 0.6$ ms and $\tau_{decay} = 31 \pm 1.6$ ms, $n = 40$ events, 2 cells (Fig. 8*A*). The E_{rev} of IPSCs was -66 ± 1 mV, a value close to E_K and similar to that obtained for ACh-evoked currents (see Fig. 1*A*).

When synaptic currents were recorded with a patch pipette containing a CsCl-BAPTA based saline solution and superfused with an external solution containing 0.5 mM Ca^{2+} plus 1 nM apamin, synaptic currents were inward at -90 mV and outward at positive voltages ($E_{rev} \approx -18$ mV). This is in agreement with observations on the isolated nAChR currents evoked by exogenously applied ACh (see Fig. 1*A*). Note that under this condition, no synaptic currents could be detected at -30 mV (Fig. 1*A*). This is due to the fact that this membrane voltage is close to E_{rev} for the nAChR and also shows that outward currents through SK channels have been effectively blocked. Consistent with the notion that the temporal course of IPSCs is governed by SK channel gating (Oliver *et al.* 2000), the kinetics of the synaptic currents studied in isolation from the SK channels at -90 mV were faster (time to peak $= 4.5 \pm 0.5$ ms, $\tau_{decay} = 20.4 \pm 1.5$ ms, $n = 41$ events, 5 cells; Figs 8*B* and *C*) than those of the combined current. The average waveform for the

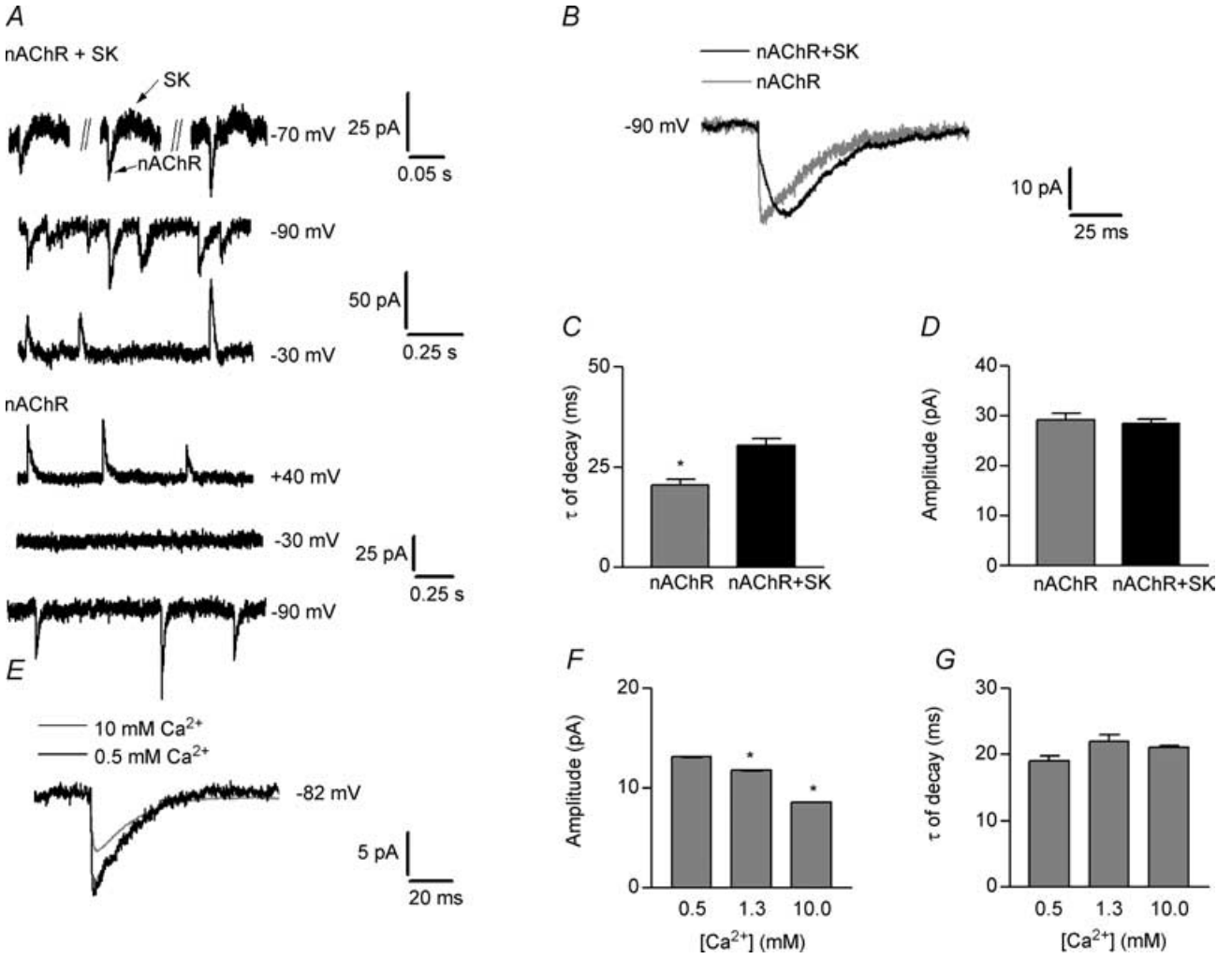

Figure 8. Ca^{2+} modulation of isolated nAChR spontaneous synaptic currents
A, representative recordings of combined (nAChR + SK) and isolated (nAChR) spontaneous synaptic currents at different voltages. Note that at -70 mV, the trace is biphasic (arrows) in the combined current records. *B*, superimposed averages of combined (black) and isolated (grey) synaptic currents. *C* and *D*, bar graphs showing τ of decay and amplitudes, respectively, of the combined nAChR + SK and isolated nAChR synaptic currents. Note that amplitudes are not significantly different whereas τ of decay is significantly faster in the isolated nAChR synaptic currents. *E*, superimposed averages of isolated synaptic currents recorded in the presence of 0.5 (black) and 10 mM (grey) Ca^{2+} in the extracellular solution. *F* and *G*, bar graphs showing that synaptic current amplitudes (*F*) are significantly reduced in the presence of 1.3 and 10 mM Ca^{2+} with respect to the amplitudes obtained in the presence of 0.5 mM Ca^{2+} and that no changes were found in τ of decay (*G*) upon varying the external Ca^{2+} concentration. All experiments were carried out in IHCs voltage clamped at -90 mV.

combined response nAChR + SK (see Fig. 8*B*) seems to have a fast and a slow component; however, it can be better fitted by one exponential and not by two. Therefore, even though in the presence of SK channels, the slowing of the synaptic current kinetics is significant, one can only speculate that the faster component seen in Fig. 8*B*, is due to the activation of the nAChR and the slower due to the opening of SK channels. Considering the effect of the presence of SK channels in the kinetics of the response, it is puzzling that no significant differences were found in the amplitude of the isolated nAChR synaptic currents with respect to that of the combined nAChR + SK IPSCs (Fig. 8*B* and *D*). At −90 mV, ionic currents through both nAChRs and SK channels are inward, but the driving force for K^+ entry is quite low ($E_K = -82$ mV), whereas the driving force for Na^+ entry through the nAChR is high ($E_{Na} = +84$ mV). Therefore, at –90 mV, under this ionic condition, the contribution of SK channels to the peak synaptic current amplitude could be very small. Nevertheless, to be able to clearly separate both components, it would be necessary to measure synaptic currents in the same cell with and without SK channels.

To evaluate whether Ca^{2+} modulates the time course and/or the amplitude of the isolated cholinergic synaptic currents through native nAChRs, we measured these parameters in IHCs voltage clamped at −82 mV (using BAPTA in the pipette solution and 1 nM apamin in the external solution) and superfused with saline solutions containing different concentrations of Ca^{2+}. We could only analyse Ca^{2+} concentrations ≥ 0.5 mM, as in lower Ca^{2+} concentrations the frequency of spontaneous currents was too low for evaluation. As illustrated by the records (Fig. 8*E*) and the bar graph (Fig. 8*F*), increasing the concentration of Ca^{2+} to 1.3 and 10 mM, caused a significant reduction (12% and 36%, respectively) in the amplitude of the nAChR synaptic currents with respect to the values obtained at 0.5 mM Ca^{2+}. Amplitudes were -13.3 ± 0.3, -11.8 ± 0.3 and -8.6 ± 0.1 pA in 0.5 ($n = 95$ events, 5 cells), 1.3 ($n = 106$ events, 5 cells, $P < 0.05$) and 10 mM ($n = 791$ events 5 cells, $P < 0.001$) Ca^{2+}, respectively. No significant differences were found in the decay time constants at the different Ca^{2+} concentrations: $\tau_{decay} = 19 \pm 0.8$, 22 ± 1 and 21 ± 0.3 ms for 0.5, 1.3 and 10 mM Ca^{2+} (Fig. 8*G*). These results are consistent with the earlier interpretation (Katz *et al.* 2000; Weisstaub *et al.* 2002) that divalent cations reduce ionic current by acting as blocking particles in the open channel. This hypothesis also accords with the observation of voltage-dependent rectification produced by Ba^{2+} (see Fig. 7).

Discussion

The main goal of the present work was to characterize, from a pharmacological and biophysical standpoint, the receptor mediating cholinergic synaptic effects on IHCs prior to the onset of hearing. Even though this is a transient synapse present in IHCs at an immature stage of cochlear development, it is functional as of postnatal day 3 (P3) to P13–14 (Glowatzki & Fuchs, 2000; Katz *et al.* 2004) and, as in other hair cells (Fuchs & Murrow, 1992*a*,*b*; Doi & Ohmori, 1993; Blanchet *et al.* 1996; Dulon & Lenoir, 1996; Evans, 1996; Fuchs, 1996; Nenov *et al.* 1996*b*; Dulon *et al.* 1998; Oliver *et al.* 2000), it is mediated by a nAChR probably composed of both the α9 and α10 subunits (see Elgoyhen *et al.* 1994, 2001). The activation of the α9α10-containing nAChR has been shown to be always coupled to the activation of the SK channels that hyperpolarize the hair cell (Glowatzki & Fuchs, 2000; Katz *et al.* 2004; Marcotti *et al.* 2004). In addition, it has been demonstrated that the presence of a functional nAChR channel depends on the presence of both the α9 and α10 subunits and that the expression of both the α10 subunit and the associated SK channels are down-regulated in IHCs after the onset of hearing, a time at which direct efferent contacts to IHCs start to retract, and cholinergic sensitivity disappears from these cells (Katz *et al.* 2004).

The characterization of the native nAChR was done in isolation from the associated SK channel in order to compare its characteristics to those of the recombinant α9 and α9α10 nAChRs expressed in *Xenopus* oocytes. The pharmacological profile and Ca^{2+} permeability of the native IHC nAChR were found to be identical to those described for both the α9 and α9α10 recombinant nAChRs. However, when comparing other biophysical characteristics, the native IHC nAChR resembles more closely the heteromeric α9α10 nAChR. Of particular interest is the observation that the native nAChRs, like heteromeric α9α10 receptors, possess two calcium binding sites. An extracellular site that facilitates ligand gating of the channel is present in both native nAChRs and heteromeric α9α10 receptors, but absent from homomeric α9 receptors expressed in *Xenopus* oocytes. However, native nAChRs IHC, heteromeric α9α10 and homomeric α9 nAChRs alike demonstrate open channel block by divalent cations (Katz *et al.* 2000; Elgoyhen *et al.* 2001; Weisstaub *et al.* 2002). Thus, comparisons of conserved and varying sequences in the α9 and α10 subunits should offer important clues to the structural bases for these functional differences.

Voltage sensitivity, pharmacological profile and desensitization pattern of the native IHC nAChR

The reversal potential and voltage sensitivity of the isolated nAChR current are consistent with those reported for the recombinant heteromeric α9α10 nAChRs expressed in *Xenopus* oocytes (Elgoyhen *et al.* 2001; Weisstaub *et al.* 2002) and for the ACh-evoked current in isolated adult guinea pig OHCs (Blanchet *et al.* 1996), developing rat OHCs (Dulon & Lenoir, 1996), short

chick hair cells (McNiven *et al.* 1996) and developing rat IHCs (Glowatzki & Fuchs, 2000). The *I–V* relationship of the IHC nAChR presents, as those of the $\alpha9$ and $\alpha9\alpha10$ recombinant nAChRs (Elgoyhen *et al.* 2001), considerable rectification around the reversal potential. However, this *I–V* differs from that of the recombinant $\alpha9$ mainly in the fact that the native nAChR, as shown for the recombinant $\alpha9\alpha10$ nAChR (Elgoyhen *et al.* 2001; Weisstaub *et al.* 2002; Sgard *et al.* 2002) can pass a considerable amount of current in the hyperpolarized direction. Conversely, currents through the $\alpha9$ nAChR at hyperpolarized potentials are potently blocked by Ca^{2+} (IC_{50} 100 μM) (Katz *et al.* 2000). This difference could be accounted for by the fact that Ca^{2+} only blocks the $\alpha9$ nAChR whereas it both potentiates and blocks the native and the heteromeric $\alpha9\alpha10$ nAChR receptors within the same range of physiological concentrations: at a concentration of 0.5 mM potentiation predominates whereas at higher Ca^{2+} concentrations, blockade starts to be apparent (see discussion below). This hypothesis is reinforced by the fact that the *I–V* curve in the presence of 5 mM Ba^{2+} has the same shape (outwardly rectifying) as that reported for $\alpha9$ in 1.8 mM Ca^{2+} (Katz *et al.* 2000; Elgoyhen *et al.* 2001). A similar outward rectification was obtained with the recombinant $\alpha9\alpha10$ nAChR upon elevating the concentration of Ca^{2+} to 3 mM (Weisstaub *et al.* 2002).

The pharmacological characteristics of the native IHC nAChR are indistinguishable from those of the recombinant $\alpha9$ and $\alpha9\alpha10$ nAChRs and also similar to those reported for the native OHCs cholinergic receptor (Elgoyhen *et al.* 1994, 2001; Erostegui *et al.* 1994*b*; Chen *et al.* 1996; Rothlin *et al.* 1999; Verbitsky *et al.* 2000). Namely, the IHC cholinergic receptor is blocked by nicotine as well as by antagonists of non-cholinergic receptors such as strychnine (glycine receptors), bicuculline (γ-aminobutyric acid type A receptors), and ICS-205930 (ligand gated serotonin receptors).

The apparent affinity of the IHC nAChR for ACh ($EC_{50} = 60.7$ μM) is somewhat lower than that reported (EC_{50} 7–30 μM) for both the recombinant $\alpha9$ and $\alpha9\alpha10$ (Elgoyhen *et al.* 1994, 2001; Weisstaub *et al.* 2002; Sgard *et al.* 2002) and the native hair cell nAChRs (Blanchet *et al.* 1996; Chen *et al.* 1996; Dulon & Lenoir, 1996; Erostegui *et al.* 1994*c*; Fuchs & Murrow, 1992*a*,*b*; Housley & Ashmore, 1991; McNiven *et al.* 1996). However, it is higher than the apparent affinity ($EC_{50} = 122$ μM) reported by Blanchet *et al.* (2000) for the nAChR of guinea pig OHCs. Several factors could account for this rather wide range of EC_{50} values: species differences, the type of preparation used (oocytes, isolated hair cells, cochlear coil), combined nAChR + SK *versus* isolated nAChR (see Blanchet *et al.* 2000) and also a very important source of variations could be the ionic composition of the external and internal solutions used to evaluate this parameter. Resolution of these issues must await further work with the isolated nAChR in IHCs and OHCs from different species, studied under the same ionic conditions.

Desensitization in the presence of the agonist is a widespread feature of ligand-gated channels (Jones & Westbrook, 1996). In the case of nAChRs, it has been shown that subunit composition alters the degree to which desensitization takes place (Fenster *et al.* 1997; Gerzanich *et al.* 1998). In agreement with this, we have shown that the homomeric $\alpha9$ nAChR does not significantly desensitize either upon the continued or intermittent presence of ACh, whereas currents through the $\alpha9\alpha10$ recombinant receptor are strongly diminished in both experimental situations (Elgoyhen *et al.* 2001). We now show that the IHC nAChR markedly desensitizes when exposed to ACh over the same time periods, thus resembling the $\alpha9\alpha10$ nAChRs. Cholinergic responses in mammalian OHCs were also shown to desensitize in the presence of ACh (Blanchet *et al.* 1996; Dulon & Lenoir, 1996; Evans, 1996; Nenov *et al.* 1996*a*).

Calcium permeability of the native IHC nAChR

A key step for the cholinergic inhibition of cochlear hair cells is the activation of calcium-dependent SK channels by an increase in cytoplasmic calcium (Fuchs, 1996; Glowatzki & Fuchs, 2000; Oliver *et al.* 2000). The high calcium permeability of the native IHC receptor found in the present work is consistent with this physiological role. This result is also in line with previous work on both chick short hair cells (Fuchs & Murrow, 1992*a*; McNiven *et al.* 1996) and rodent OHCs (Blanchet *et al.* 1996) that has shown evidence that the hair cell receptor must have a considerable Ca^{2+} permeability. It should be remembered, however, that Ca^{2+} blocks the total inward current, composed of Na^+ and Ca^{2+}, through the IHC nAChR. This interaction violates the principle of ionic independence assumed by the Goldman-Hodgkin-Katz formalism and therefore the values obtained for relative permeabilities should be taken only as estimates to compare to the values obtained for the $\alpha9$ and $\alpha9\alpha10$ recombinant receptors (Katz *et al.* 2000; Elgoyhen *et al.* 2001; Weisstaub *et al.* 2002; Sgard *et al.* 2002) and to other recombinant and native ligand-gated channels.

The present P_{Ca}/P_{Na} estimated for the IHC nAChR, however, is of about one order of magnitude lower than that obtained by Jagger *et al.* (2000) for the nAChR present in hair cell precursor lines from the immortomouse. The source of this discrepancy is not clear. However, aside from the fact that channels could behave differently in a cell line, one possible explanation could be that the nAChR of the immortomouse hair cells might have a different nAChR subunit composition and/or stoichiometry from those of rat cochlear hair cells.

The high Ca^{2+} permeability of the native IHC nAChR estimated in the present study (P_{Ca}/P_{Na} ~8) is similar to that reported for the homomeric $\alpha9$ and the heteromeric $\alpha9\alpha10$ nAChRs (Katz *et al.* 2000; Weisstaub *et al.* 2002) and is also in the same range as that of the homomeric $\alpha7$ nAChR (P_{Ca}/P_{Na} ~10–20) (Bertrand *et al.* 1990; Sands & Barish, 1991; Séguéla *et al.* 1993; Katz *et al.* 2000), highest among all nAChRs. The P_{Ca}/P_{Na} of this group of nAChRs is similar to that of other ligand-gated channels with high Ca^{2+} permeability, such as the NMDA receptors and cyclic nucleotide-gated channels (Mayer & Westbrook, 1987; Frings, 1997). As for the hair cell nAChR, in many cases the main role of these calcium-permeable receptors is not that of depolarizing the membrane, but rather to trigger cellular functions through Ca^{2+} entry into the cell (Burnashev, 1998).

Effects of divalent cations on the isolated IHC nAChR currents

Modulation by external Ca^{2+}, which can vary dramatically in concentration during high synaptic activity (Brown *et al.* 1995), is a widespread feature of both recombinant and native nAChRs. The tight modulation of the IHC nAChR by extracellular Ca^{2+} resembles what has been described for the $\alpha9\alpha10$ receptor where Ca^{2+} potentiates ACh responses in the micromolar range and blocks them at concentrations > 0.5 mM (Weisstaub *et al.* 2002). Studies performed in chick short hair cells show that the native avian cholinergic receptor is also biphasically modulated by Ca^{2+}, but the range of concentrations at which modulation is observed in that preparation was significantly higher (McNiven *et al.* 1996). In isolated mammalian OHCs loaded with internal BAPTA, ACh-evoked currents at +32 mV were strongly reduced, and almost completely abolished at –81 mV, by removal of external Ca^{2+} (Blanchet *et al.* 1996). However, in those experiments Ca^{2+} was replaced with Mg^{2+}, which potently blocks the recombinant $\alpha9\alpha10$ nAChR (Weisstaub *et al.* 2002) and, as we show here, the native IHC nAChR. A similar biphasic effect of Ca^{2+} on the IHC nAChR was recently reported (Marcotti *et al.* 2004), although that involved both cation current through the nAChR and the accompanying SK current. Therefore, although the results were qualitatively similar, the interpretation was restricted by that additional complexity.

As reported for the $\alpha9\alpha10$ nAChR (Weisstaub *et al.* 2002) and for other nAChRs (Ifune & Steinbach, 1991; Mulle *et al.* 1992*b*; Booker *et al.* 1998; Liu & Berg, 1999), micromolar Ba^{2+}, but not Mg^{2+}, mimicked the enhancing effects of Ca^{2+} on the IHC nAChR. The effects of Ba^{2+} on ACh-evoked currents have been previously studied in guinea pig OHCs (Erostegui *et al.* 1994*a*). In that case, however, the authors did not see any ACh-activated current when they replaced extracellular Ca^{2+} by Ba^{2+}. The discrepancy with the present results might be accounted for by the fact that: (1) they were looking at the combined nAChR + SK currents and evaluated the effects of Ba^{2+} at 0 mV, near the reversal potential for current through the nAChR, and (2) Ba^{2+} is both a poor activator and a blocker of SK channels (Soh & Park, 2001), making the outward currents through SK negligible. As reported for OHCs (Nenov *et al.* 1996*b*), Mg^{2+} also blocked currents through the native IHC nAChR at physiological concentrations. Therefore, the effects of OC efferent activation on IHCs will depend not only on the external Ca^{2+} concentration, but on the Ca^{2+}/Mg^{2+} ratio in the perilymph. It remains uncertain why Mg^{2+} does not potentiate responses of ACh on IHCs. Mg^{2+} has a smaller metallic radius (150 pm) than Ca^{2+} and Ba^{2+} (180 and 215 pm, respectively). As charge density is greater in Mg^{2+} than in Ba^{2+} and Ca^{2+}, the interaction between either Ca^{2+} or Ba^{2+} with a H_2O molecule would be weaker than that of Mg^{2+}. Thus, as postulated for $\alpha7$ nAChRs, the difference in the actions of these divalent cations could possibly be due to the fact that Mg^{2+} has a higher charge density than Ca^{2+} and Ba^{2+} resulting in a larger hydration radio and a slower dehydration rate, which may prevent this divalent cation from interacting with the sites involved in potentiation (Eddins *et al.* 2002).

Mechanism of Ca^{2+} potentiation and block

Calcium potentiates nAChRs through allosteric effects at an extracellular site (Decker & Dani, 1990; Mulle *et al.* 1992*b*; Vernino *et al.* 1992; Galzi *et al.* 1996) and is independent both from Ca^{2+} influx and membrane potential (Mulle *et al.* 1992*b*; Vernino *et al.* 1992; Weisstaub *et al.* 2002). Likewise, gating of the hair cell's nAChR was enhanced even when cytoplasmic calcium was heavily buffered with BAPTA. The fact that Ca^{2+} caused a leftward shift in the ACh concentration–response curve, indicates that potentiation by Ca^{2+} involves changes in the apparent affinity of the native IHC receptor for ACh. A change in the apparent affinity could imply changes in agonist binding, in the cooperativity of the system, in the coupling between agonist binding and channel gating and/or changes in the kinetic properties of these receptors. Increased agonist binding seems less likely as it has been reported that Ca^{2+} is a competitive inhibitor of *Torpedo* nAChRs in the 0.1–1 mM range, and therefore increasing Ca^{2+} from 0 to 0.5 mM would decrease ACh occupancy of the binding site (Chang & Neumann, 1976). Cooperativity of ACh binding in hippocampal nAChRs is altered by extracellular Ca^{2+} levels (Bonfante-Cabarcas *et al.* 1996), but we did not find significant differences in the Hill coefficients of the concentration–response curves to ACh obtained in the presence or absence of Ca^{2+}. Changes in the kinetic properties of the receptors by Ca^{2+}, leading to increases in the probability or the frequency of channel opening, have been previously shown for other nAChRs (Mulle *et al.*

1992*b*; Amador & Dani, 1995). However, further analysis would be needed to prove this hypothesis.

The voltage dependence of Ba^{2+} block suggests that, as reported for the recombinant homomeric $\alpha 9$ and heteromeric $\alpha 9\alpha 10$ receptors (Katz *et al.* 2000; Weisstaub *et al.* 2002), the site of action of either Ca^{2+} or Ba^{2+} might lie within the channel pore and might involve hindering the passage of Na^{+} through the channel in the presence of divalent cations. This was also suggested for neuronal and muscle nAChRs (Decker & Dani, 1990; Mulle *et al.* 1992*a*,*b*) and for other ligand-gated and mechanosensitive channels (Frings *et al.* 1995; Ricci & Fettiplace, 1998).

Ca^{2+} modulates nAChR spontaneous synaptic currents

The modulatory effects of Ca^{2+} were also seen on spontaneous synaptic currents which result from ACh released by efferent synaptic terminals contacting the IHCs (Glowatzki & Fuchs, 2000; Katz *et al.* 2004). Elevating Ca^{2+} from 0.5 mM to 1.3 and 10 mM significantly decreased the amplitude of synaptic currents without affecting their time course. The reduction in amplitude is in agreement with, although less pronounced than, the blocking effects of Ca^{2+} on the amplitude of currents evoked by exogenous ACh. The lack of effect of external Ca^{2+} on the time course of synaptic currents is in line with the idea that Ca^{2+} potentiation of nAChRs might be due to an effect on channel gating (Mulle *et al.* 1992*b*; Amador & Dani, 1995) whereas Ca^{2+} block is most likely due to the hindering of the passage of monovalent ions through the pore (Decker & Dani, 1990; Mulle *et al.* 1992*a*,*b*; Katz *et al.* 2000; Weisstaub *et al.* 2002). Therefore, Ca^{2+} block would affect the conductance of the channels without affecting channel kinetics and hence it should not have any effect on the time course of synaptic currents. In the IHC nAChR, as well as in the recombinant $\alpha 9\alpha 10$ receptor, the potentiating effects of external Ca^{2+} are only evident at very low Ca^{2+} concentrations (0–0.5 mM). Therefore, we could not study the potentiating effects of Ca^{2+} on synaptic currents due to the extremely low number of events we found in the absence of external Ca^{2+}.

Physiological implications

In view of the high Ca^{2+} influx the native IHC nAChR can generate and the critical role Ca^{2+} plays in the inhibitory sign of this fast cholinergic synapse, it is not surprising that its activity is tightly regulated by external Ca^{2+} within physiological ranges of concentration. *In vivo*, during periods of intense synaptic activity, extracellular Ca^{2+} at the synaptic cleft could be significantly reduced (Brown *et al.* 1995) and thus provide a type of negative feedback control by decreasing receptor function. Conversely, during normal synaptic activity, with physiological concentrations of Ca^{2+} and Mg^{2+} in the perilymph (1.3 and 0.9 mM, respectively) the total current through this receptor would be reduced due to the hindering effects divalent cations have on the Na^{+} inward current. This would minimize the depolarization of the hair cell membrane upon activation of the $\alpha 9\alpha 10$ nAChR and maximize Ca^{2+} influx through the activated receptor, thus leading to the activation of SK channels that hyperpolarize the cell.

References

Amador M & Dani JA (1995). Mechanism for modulation of nicotinic acetylcholine receptors that can influence synaptic transmission. *J Neurosci* **15**, 4525–4532.

Bertrand D, Ballivet M & Rungger D (1990). Activation and blocking of neuronal nicotinic acetylcholine receptor reconstituted in *Xenopus* oocytes. *Proc Natl Acad Sci U S A* **87**, 1993–1997.

Blanchet C, Erostegui C, Sugasawa M & Dulon D (1996). Acetylcholine-induced potassium current of guinea pig outer hair cells: its dependence on a calcium influx through nicotinic-like receptors. *J Neurosci* **16**, 2574–2584.

Blanchet C, Erostegui C, Sugasawa M & Dulon D (2000). Gentamicin blocks ACh-evoked K^{+} current in guinea-pig outer hair cells by impairing Ca^{2+} entry at the cholinergic receptor. *J Physiol* **525**, 641–654.

Bonfante-Cabarcas R, Swanson KL, Alkondon M & Albuquerque EX (1996). Diversity of nicotinic acetylcholine receptors in rat hippocampal neurons. IV. Regulation by external Ca^{++} of alpha-bungarotoxin-sensitive receptor function and of rectification induced by internal Mg^{++}. *J Pharmacol Exp Ther* **277**, 432–444.

Booker TK, Smith KW, Dodrill C & Collins AC (1998). Calcium modulation of activation and desensitization of nicotinic receptors from mouse brain. *J Neurochem* **71**, 1490–1500.

Brown EM, Vassilev PM & Hebert SC (1995). Calcium ions as extracellular messengers. *Cell* **83**, 679–682.

Burnashev N (1998). Calcium permeability of ligand-gated channels. *Cell Calcium* **24**, 325–332.

Chang HW & Neumann E (1976). Dynamic properties of isolated acetylcholine receptor proteins: release of calcium ions caused by acetylcholine binding. *Proc Natl Acad Sci U S A* **73**, 3364–3368.

Chen C, LeBlanc C & Bobbin R (1996). Differences in cholinergic responses from outer hair cells of rat and guinea pig. *Hear Res* **98**, 9–17.

Decker ER & Dani JA (1990). Calcium permeability of the nicotinic acetylcholine receptor: the single-channel calcium influx is significant. *J Neurosci* **10**, 3413–3420.

Doi T & Ohmori H (1993). Acetylcholine increases intracellular Ca^{2+} concentration and hyperpolarizes the guinea-pig outer hair cell. *Hear Res* **67**, 179–188.

Dulon D & Lenoir M (1996). Cholinergic responses in developing outer hair cells of the rat cochlea. *Eur J Neurosci* **8**, 1945–1952.

Dulon D, Luo L, Zhang C & Ryan AF (1998). Expression of small-conductance calcium-activated potassium channels (SK) in outer hair cells of the rat cochlea. *Eur J Neurosci* **10**, 907–915.

Eddins D, Lyford LK, Lee JW, Desai SA & Rosenberg RL (2002). Permeant but not impermeant divalent cations enhance activation of nondesensitizing alpha7 nicotinic receptors. *Am J Physiol Cell Physiol* **282**, C796–C804.

Elgoyhen AB, Johnson DS, Boulter J, Vetter DE & Heinemann S (1994). Alpha 9: an acetylcholine receptor with novel pharmacological properties expressed in rat cochlear hair cells. *Cell* **79**, 705–715.

Elgoyhen A, Vetter D, Katz E, Rothlin C, Heinemann S & Boulter J (2001). Alpha 10: a determinant of nicotinic cholinergic receptor function in mammalian vestibular and cochlear mechanosensory hair cells. *Proc Natl Acad Sci U S A* **98**, 3501–3506.

Erostegui C, Nenov AP, Norris CH & Bobbin RP (1994*a*). Acetylcholine activates a K^+ conductance permeable to Cs^+ in guinea pig outer hair cells. *Hear Res* **81**, 119–129.

Erostegui C, Norris CH & Bobbin RP (1994*b*). In vitro characterization of a cholinergic receptor on outer hair cells. *Hear Res* **74**, 135–147.

Erostegui C, Norris CH & Bobbin RP (1994*c*). In vitro pharmacologic characterization of a cholinergic receptor on outer hair cells. *Hear Res* **74**, 135–147.

Evans MG (1996). Acetylcholine activates two currents in guinea-pig outer hair cells. *J Physiol* **491**, 563–578.

Fenster CP, Rains MF, Noerager B, Quick MW & Lester RA (1997). Influence of subunit composition on desensitization of neuronal acetylcholine receptors at low concentrations of nicotine. *J Neurosci* **17**, 5747–5759.

Frings S (1997). Cyclic nucleotide-gated channels and calcium: an intimate relation. *Adv Second Messenger Phosphoprotein Res* **31**, 75–82.

Frings S, Seifert R, Godde M & Kaupp UB (1995). Profoundly different calcium permeation and blockage determine the specific function of distinct cyclic nucleotide-gated channels. *Neuron* **15**, 169–179.

Fuchs PA (1996). Synaptic transmission at vertebrate hair cells. *Curr Opin Neurobiol* **6**, 514–519.

Fuchs PA & Murrow BW (1992*a*). Cholinergic inhibition of short (outer) hair cells of the chick's cochlea. *J Neurosci* **12**, 800–809.

Fuchs PA & Murrow BW (1992*b*). A novel cholinergic receptor mediates inhibition of chick cochlear hair cells. *Proc R Soc Lond Biol Sci* **248**, 33–40.

Galzi JL, Bertrand S, Corringer PJ, Changeux JP & Bertrand D (1996). Identification of calcium binding sites that regulate potentiation of a neuronal nicotinic acetylcholine receptor. *EMBO J* **15**, 5824–5832.

Gerzanich V, Wang F, Kuryatov A & Lindstrom J (1998). alpha 5 subunit alters desensitization, pharmacology, Ca^{++} permeability and Ca^{++} modulation of human neuronal alpha 3 nicotinic receptors. *J Pharmacol Exp Ther* **286**, 311–320.

Glowatzki E & Fuchs PA (2000). Cholinergic synaptic inhibition of inner hair cells in the neonatal mammalian cochlea. *Science* **288**, 2366–2368.

Gomez-Casati ME, Katz E, Glowatzki E, Lioudyno MI, Fuchs P & Elgoyhen AB (2004). Linopirdine blocks alpha9alpha10-containing nicotinic cholinergic receptors of cochlear hair cells. *J Assoc Res Otolaryngol* **5**, 261–269.

Guinan JJ (1996). Efferent physiology. In *The Cochlea*, ed. Dallos P, Popper AN & Fay RR, pp. 435–502. Springer, New York.

Housley GD & Ashmore JF (1991). Direct measurement of the action of acetylcholine on isolated outer hair cells of the guinea pig cochlea. *Proc R Soc Lond B Biol Sci* **244**, 161–167.

Ifune CK & Steinbach JH (1991). Voltage-dependent block by magnesium of neuronal nicotinic acetylcholine receptor channels in rat phaeochromocytoma cells. *J Physiol* **443**, 683–701.

Jagger DJ, Griesinger CB, Rivolta MN, Holley MC & Ashmore JF (2000). Calcium signalling mediated by the 9 acetylcholine receptor in a cochlear cell line from the Immortomouse. *J Physiol* **527**, 49–54.

Jan LY & Jan YN (1976). L-Glutamate as an excitatory transmitter at the *Drosophila* larval neuromuscular junction. *J Physiol* **262**, 215–236.

Jones MV & Westbrook GL (1996). The impact of receptor desensitization on fast synaptic transmission. *Trends Neurosci* **19**, 96–101.

Katz E, Elgoyhen AB, Gomez-Casati ME, Knipper M, Vetter DE, Fuchs PA & Glowatzki E (2004). Developmental regulation of nicotinic synapses on cochlear inner hair cells. *J Neurosci* **24**, 7814–7820.

Katz E, Verbitsky M, Rothlin CV, Vetter DE, Heinemann SF & Belen Elgoyhen A (2000). High calcium permeability and calcium block of the alpha9 nicotinic acetylcholine receptor. *Hear Res* **141**, 117–128.

Kohler M, Hirschberg B, Bond CT, Kinzie JM, Marrion NV, Maylie J & Adelman JP (1996). Small-conductance, calcium-activated potassium channels from mammalian brain. *Science* **273**, 1709–1714.

Köler M, Hirshberg B, Bond CT, Kinzie JM, Marrion NV, Maylie J & Adelman JP (1996). Small-conductance, calcium-activated potassium channels from mammalian brain. *Science* **273**, 1709–1714.

Kros CJ, Ruppersberg JP & Rusch A (1998). Expression of a potassium current in inner hair cells during development of hearing in mice. *Nature* **394**, 281–284.

Lioudyno M, Hiel H, Kong JH, Katz E, Waldman E, Parameshwaran-Iyer S, Glowatzki E & Fuchs PA (2004). A 'synaptoplasmic cistern' mediates rapid inhibition of cochlear hair cells. *J Neurosci* **24**, 11160–11164.

Liu QS & Berg DK (1999). Extracellular calcium regulates responses of both alpha3- and alpha7-containing nicotinic receptors on chick ciliary ganglion neurons. *J Neurophysiol* **82**, 1124–1132.

Luo L, Bennett T, Jung HH & Ryan A (1998). Developmental expression of alpha 9 acetylcholine receptor mRNA in the rat cochlea and vestibular inner ear. *J Comp Neurol* **393**, 320–331.

Marcotti W, Johnson SL & Kros CJ (2004). A transiently expressed SK current sustains and modulates action potential activity in immature mouse inner hair cells. *J Physiol* **560**, 691–708.

Mayer M & Westbrook G (1987). Permeation and block of *N*-methyl-D-aspartic acid receptor channels by divalent cations in mouse cultured central neurones. *J Physiol* **394**, 501–527.

McNiven AI, Yuhas WA & Fuchs PA (1996). Ionic dependence and agonist preference of an acetylcholine receptor in hair cells. *Auditory Neurosci* **2**, 63–77.

Morley BJ, Li HS, Hiel H, Drescher DG & Elgoyhen AB (1998). Identification of the subunits of the nicotinic cholinergic receptors in the rat cochlea using RT-PCR and in situ hybridization. *Brain Res Mol Brain Res* **53**, 78–87.

Morley BJ & Simmons DD (2002). Developmental mRNA expression of the alpha10 nicotinic acetylcholine receptor subunit in the rat cochlea. *Brain Res Dev Brain Res* **139**, 87–96.

Mulle C, Choquet D, Korn H & Changeux JP (1992*a*). Calcium influx through nicotinic receptors in rat central neurons: its relevance to cellular regulation. *Neuron* **8**, 135–143.

Mulle C, Lena C & Changeux JP (1992*b*). Potentiation of nicotinic receptor response by external calcium in rat central neurons. *Neuron* **8**, 937–945.

Nenov AP, Norris C & Bobbin RP (1996*a*). Acetylcholine response in guinea pig outer hair cells. I. Properties of the response. *Hear Res* **101**, 132–148.

Nenov AP, Norris C & Bobbin RP (1996*b*). Acetylcholine responses in guinea pig outer hair cells. II. Activation of a small conductance Ca^{2+}-activated K^+ channel. *Hear Res* **101**, 149–172.

Oliver D, Klocker N, Schuck J, Baukrowitz T, Ruppersberg JP & Fakler B (2000). Gating of Ca^{2+}-activated K^+ channels controls fast inhibitory synaptic transmission at auditory outer hair cells. *Neuron* **26**, 595–601.

Park H, Niedzielski AS & Wenthold RJ (1997). Expression of the nicotinic acetylcholine receptor subunit, a9, in the guinea pig cochlea. *Hear Res* **112**, 95–105.

Pujol R, Lavigne-Rebillard M & Lenoir M (1998). Development of sensory and neural structures in the mammalian cochlea. In *Development of the Auditory System*, ed. Rubel EW, Popper AN & Fay RR, pp. 146–192. Springer-Verlag, New York.

Ricci AJ & Fettiplace R (1998). Calcium permeation of the turtle hair cell mechanotransducer channel and its relation to the composition of endolymph. *J Physiol* **506**, 159–173.

Rothlin CV, Katz E, Verbitsky M & Elgoyhen AB (1999). The alpha9 nicotinic acetylcholine receptor shares pharmacological properties with type A gamma-aminobutyric acid, glycine, and type 3 serotonin receptors. *Mol Pharmacol* **55**, 248–254.

Sands SB & Barish ME (1991). Calcium permeability of neuronal nicotinic acetylcholine receptor channels in PC12 cells. *Brain Res* **560**, 38–42.

Séguéla P, Wadiche J, Dineley-Miller K, Dani JA & Patrick JW (1993). Molecular cloning, functional properties, and distribution of rat brain α7: a nicotinic cation channel highly permeable to calcium. *J Neurosci* **13**, 596–604.

Sgard F, Charpentier E, Bertrand S, Walker N, Caput D, Graham D, Bertrand D & Besnard F (2002). A novel human nicotinic receptor subunit, α10, that confers functionality to the α9-subunit. *Mol Pharmacol* **61**, 150–159.

Simmons DD, Moulding HD & Zee D (1996). Olivocochlear innervation of inner and outer hair cells during postnatal maturation: an immunocytochemical study. *Brain Res Dev Brain Res* **95**, 213–226.

Soh H & Park CS (2001). Inwardly rectifying current-voltage relationship of small-conductance Ca^{2+}-activated K^+ channels rendered by intracellular divalent cation blockade. *Biophys J* **80**, 2207–2215.

Verbitsky M, Rothlin C, Katz E & Elgoyhen AB (2000). Mixed nicotinic-muscarinic properties of the α9 nicotinic receptor. *Neuropharmacol* **39**, 2515–2524.

Vernino S, Amador M, Luetje CW, Patrick J & Dani JA (1992). Calcium modulation and high calcium permeability of neuronal nicotinic acetylcholine receptors. *Neuron* **8**, 127–134.

Vetter DE, Liberman MC, Mann J, Barhanin J, Boulter J, Brown MC, Saffiote-Kolman J, Heinemann SF & Elgoyhen AB (1999). Role of alpha9 nicotinic ACh receptor subunits in the development and function of cochlear efferent innervation. *Neuron* **23**, 93–103.

Walsh E, McGee J, McFadden S & Liberman M (1998). Long-term effects of sectioning the olivocochlear bundle in neonatal cats. *J Neurosci* **18**, 3859–3869.

Weisstaub N, Vetter DE, Elgoyhen AB & Katz E (2002). The alpha9alpha10 nicotinic acetylcholine receptor is permeable to and is modulated by divalent cations. *Hear Res* **167**, 122–135.

Acknowledgements

This work was supported by an International Research Scholar Grant from the Howard Hughes Medical Institute, a Research Grant from ANPCyT (Argentina) to A.B.E., a Research grant from Universidad de Buenos Aires (Argentina) to A.B.E and E.K., a Research Grant from CONICET (Argentina) to E.K., a National Institutes of Health Research Grant RO3TW006247 to P.A.F and A.B.E. (E.K. Associate Investigator) from the Fogarty International Center and by a National Institutes of Deafness and other Communication Disorders (NIDCD) Grant R01DC01508 to P.A.F., A.B.E and E.K. (co-investigator). We want to thank Dr Elisabeth Glowatzki for her generous and continued support of our work. We also want to thank Dr Alejandro Paladini for technical assistance with the electronic equipment and Mr Norberto Malarini for his expert assistance in the purchase of imported equipment and laboratory supplies.